Available online at www.sciencedirect.com
ScienceDirect
Trans. Nonferrous Met. Soc. China 25(2015) 1763−1769
Transactions of Nonferrous Metals Society of China
www.tnmsc.cn

Microstructure and properties of Al−0.70Fe−0.24Cu alloy conductor prepared by horizontal continuous casting and subsequent continuous extrusion forming

Xiao-yuan ZHANG[1], Hui ZHANG[1,2], Xiang-xin KONG[1], Ding-fa FU[1,2]

1. College of Materials Science and Engineering, Hunan University, Changsha 410082, China;
2. Key Laboratory for Spray Deposition Technology and Application of Hunan Province, Hunan University, Changsha 410082, China

Received 13 July 2014; accepted 13 November 2014

Abstract: A novel process for manufacturing Al−0.70Fe−0.24Cu alloy conductor was proposed, which includes horizontal continuous casting and subsequent continuous extrusion forming (Conform). The mechanical properties, electrical conductivity and the compressed creep behaviour of the alloy were studied. The results indicate that the Conform process induces obvious grain refinement, strain-induced precipitation of Al_7Cu_2Fe phase and the transformation of crystal orientation distribution. The processed alloy has good comprehensive mechanical properties and electrical conductivity. Moreover, a better creep resistance under the conditions of 90 °C and 76 MPa is shown compared with pure Al and annealed copper, and the relationship between primary creep strain and time may comply with the logarithmic law. The enhanced properties are attributed to the grain refinement as well as the fine and homogeneously distributed thermally stable AlFe and Al_7Cu_2Fe precipitation phases.

Key words: Al−0.70Fe−0.24Cu alloy; horizontal continuous casting; continuous extrusion forming; microstructure; property

1 Introduction

Al−Fe−Cu alloy conductor offers significant advantages such as light mass, high electrical conductivity, good creep resistance and good corrosion resistance by adding alloy elements Fe, Cu, Mg, etc., which is also not subject to the junction failure that occurs to the pure Al conductor. Thus, it has been an alternative of the copper and widely used for urban building cable wires [1,2].

Conventionally, the continuous casting and rolling (CC&R) process has been used in producing various non-ferrous rods, wires and sheets, and Al conductors as well [3]. The molten metal pouring into the rotary mould wheel is cast to a bar, and then the cast bar is hot-rolled to the coiled rod through a series of rolling mill stands. However, there are still many difficulties in producing commercial hard-aluminum alloy wire and rod by the continuous casting and rolling process.

The horizontal continuous casting (HCC) has been widely employed in casting nonferrous metals, such as Al, Mg, and Zn, owing to its characteristic features such as low investment cost, low energy consumption, high productivity and high quality ingot with good surface [4,5]. The continuous extrusion forming process, namely the Conform process, has been most widely used in the efficient continuous production of Al alloys and other metals due to its superiorities of energy saving, high extrusion ratio and production efficiency, large length, and high homogeneity [6]. During Conform process, the feed stock is fed into the profiled groove of the Conform wheel by a coining roll and the groove is closed by a close fitting shoe. The material is prevented from continuing its passage around the wheel by an abutment. As a result, high temperatures and pressures are developed in the material which becomes plastic and finally emerges from the machine through an extrusion die. The Conform process can produce various forms of products including tubes, solids, complex profiles and coaxial products [7,8].

In the present work, a new method to manufacture Al−0.70Fe−0.24Cu alloy conductor including the horizontal continuous casting (HCC) and subsequent

Foundation item: Project (20130161110007) supported by the Doctoral Program of Higher Education of China
Corresponding author: Hui ZHANG; Tel: +86-731-88664086; Fax: +86-731-88821483; E-mail: zhanghui63hunu@163.com; zhanghui63@hnu.edu.cn
DOI: 10.1016/S1003-6326(15)63781-5

Conform process was proposed. Figure 1 shows the principle schematic diagram of the novel method. The microstructure, mechanical properties, electrical conductivity and compressed creep behavior of the alloy were studied.

2 Experimental

The experiments were performed on Al−0.70Fe−0.24Cu alloy rods with a diameter of 12 mm prepared by the horizontal continuous casting (HCC), and the chemical compositions were 0.70% Fe, 0.24% Cu, 0.03% Mg, 0.07% Si, 0.009% B and balance Al (mass fraction). Then, the cast-rods were cleaned and extruded to coiled material with a diameter of 9.5 mm on an LJ300 continuous extrusion forming machine with a wheel revolving speed of 22 r/min and a die exit temperature of about 430 °C. After extrusion, the extruded materials were water-cooled at about 2 m away from the die exit.

The tensile specimens with a gauge length of 30 mm and a diameter of 6 mm were machined from the horizontal continuous casting rods and the extruded conductors. The tensile tests were performed on a computer-controlled INSTRON 3382 universal testing machine at a constant strain rate of 1×10^{-3} s^{-1}. The compressed creep tests were performed at 90 ºC and a constant load stress of 76 MPa for 100 h with the specimens of 9.0 mm in diameter and 25 mm in gauge length. The testing temperature fluctuations along the gauge length were controlled within ±1 °C. All the data were recorded by a computer. The electrical conductivities of HCC and Conform processed specimens were measured by a custom-made four-point probe system with four electrical contacts on the cleaned sample surface. The X-ray diffraction (XRD) patterns were recorded by the Siemens D5000 diffractometer system with monochromated Cu K_α radiation operating at 40 kV and 300 mA. The sampling width and scanning speed were fixed at 0.04° and 5.00 (°)/min, respectively. The microstructures of the initial HCC and the Conform processed Al−0.70Fe−0.24Cu alloy samples, as well as the creep specimens, crept for 20, 40 and 100 h, respectively, were characterized by an optical microscope (OM), an FEI QUANTA200 scanning electron microscope (SEM) and a JEM−3010 transmission electron microscope (TEM).

3 Results and discussion

3.1 Microstructure of HCC Al−0.70Fe−0.24Cu alloy

Figures 2 and 3 show the initial microstructures in the core of the HCC Al−0.70Fe−0.24Cu alloy. The columnar coarse grains with 60−80 μm in length and 15−20 μm in width as well as some small equiaxed grains (5−10 μm) are observed on the transverse section. The bimodal distribution of grains is also observed on the longitudinal section, and some coarse columnar grains are interspersed with massive fine equiaxed grains (3−5 μm). The difference of grain size between the transverse section and the longitudinal section may be related to the thermal dissipation condition during the HCC (Fig. 1).

Owing to impurity atoms concentrating on the grain boundaries during solidification, grain boundary segregation is observed in Figs. 3(a) and (b) as well. Irregular eutectic phases such as reticular needle-like or rod-like are distributed along grain boundaries. Moreover, there are some fine particles in the grain interior.

The EDS analysis (Table 1) indicates that the irregular eutectic phases are Fe-rich intermetallic compounds, and interior fine particles are Al−Fe−Mg phase. By combining the EDS results with the XRD results (Fig. 4), two or more kinds of phases may distribute in the grain interior and at the grain boundaries.

The XRD patterns of the HCC Al−0.70Fe−0.24Cu alloy on both the transverse section and the longitudinal

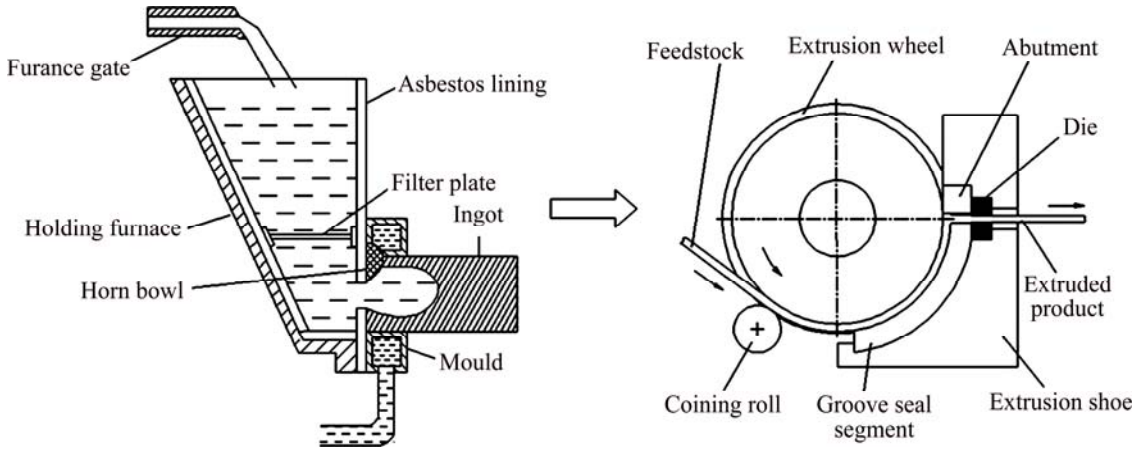

Fig. 1 Schematic illustrations of HCC and Conform process

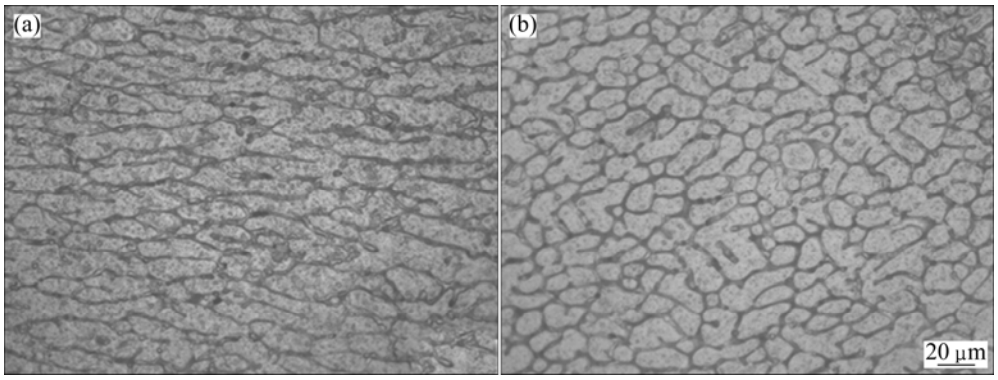

Fig. 2 Optical micrographs in core of HCC Al−0.70Fe−0.24Cu alloy: (a) Transverse section; (b) Longitudinal section

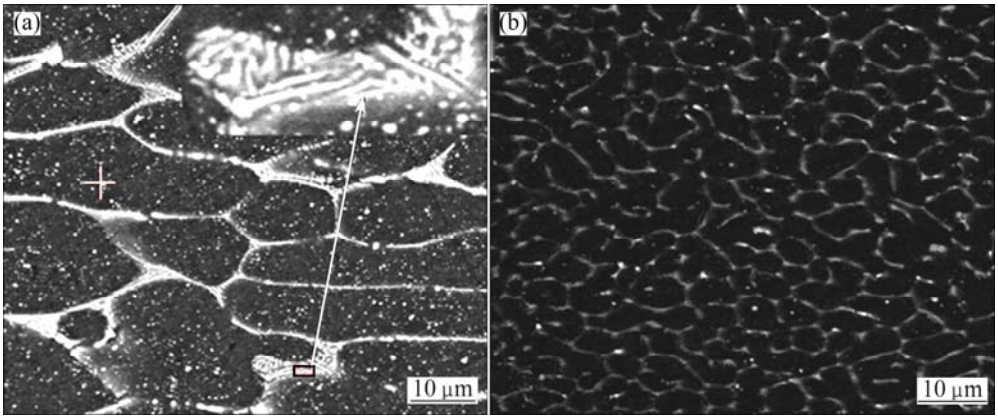

Fig. 3 SEM images in core of HCC Al−0.70Fe−0.24Cu alloy: (a) Transverse section; (b) Longitudinal section

Table 1 EDS results of HCC Al−0.70Fe−0.24Cu alloy

Area	Mole fraction/%		
	Al	Fe	Mg
Phase along grain boundary	89.83	10.17	0
Phase in grain interior	98.19	0.58	1.23

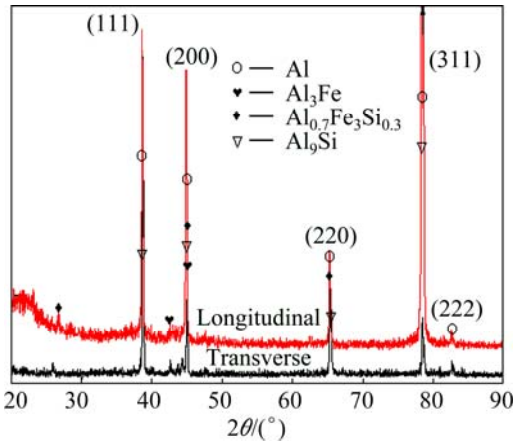

Fig. 4 XRD patterns of HCC Al−0.70Fe−0.24Cu alloy on transverse and longitudinal sections

section are shown in Fig. 4. Due to the finer grains on the longitudinal section compared with those on the transverse section (Fig. 2), the relative X-ray peak intensity on the longitudinal section is more intense than that on the transverse section. The maximum intensity of Al peak changes from crystallographic plane (111) on the transverse section to crystallographic plane (311) on the longitudinal section, which indicates that the crystal orientation distributions are different on the transverse and longitudinal sections.

3.2 Microstructure and properties of Conform processed Al−0.70Fe−0.24Cu alloy

The optical microstructures of the longitudinal section obtained from the center area of the Conform processed Al−0.70Fe−0.24Cu alloy conductor are shown in Fig. 5. There is an obvious change of grain morphology after the Conform process (Fig. 5) compared with that of the HCC (Fig. 2(b)). A more homogeneously distributed and finer-grained structure can be found in the Conform processed Al−0.70Fe−0.24Cu alloy. And the grain size reduces to the level of 5 μm. The degree of segregation decreases significantly (Fig. 5(c)) compared with the microstructure of HCC (Fig. 3(a)). This is probably related to the deformation and temperature characteristics of the metal during the Conform process [6]. In the Conform process, the intense internal shear band (IISB) and temperature evolution from room to extrusion temperatures are considered to exist in the deformation zone [7]. The IISB reduces the unevenness

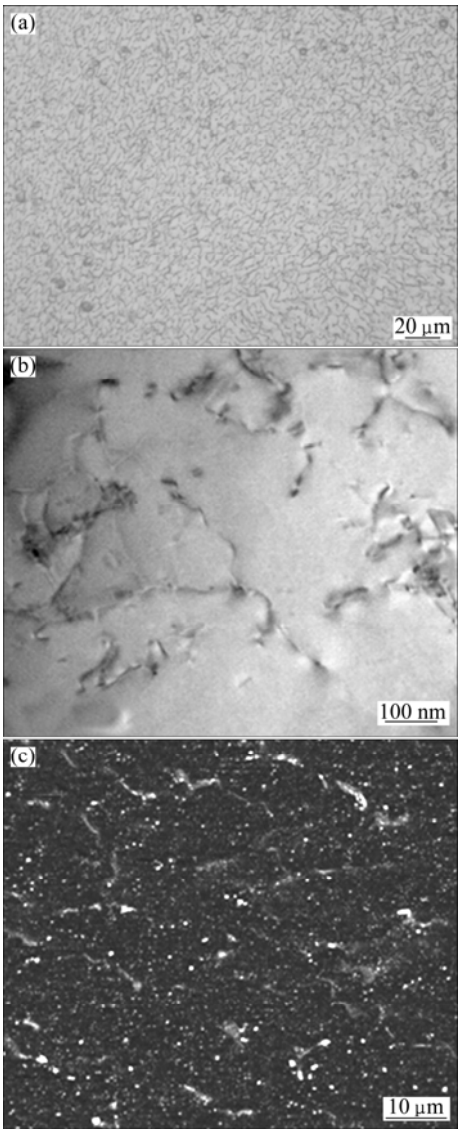

Fig. 5 Microstructures of Conform processed Al−0.70Fe−0.24Cu alloy: (a) OM; (b) TEM; (c) SEM

of plastic deformation, and is beneficial to improving the plastic deformation of the Al−0.70Fe−0.24Cu alloy. The accumulation of dislocations at the temperature-rise stage leads to ample deformation stored energy which can accelerate dynamic recovery (DRV) and even dynamic recrystallization (DRX) [6] during Conform deformation and static recovery (SRV) and static recrystallization (SRX) happening at the interval between the die exit and cooling, resulting in refined grains and uniform distribution (Fig. 5(a)).

Moreover, the primary phases of the Conform processed Al−0.70Fe−0.24Cu alloy can be demonstrated by the XRD results in Fig. 6, indicating that the Conform process induces the precipitation of Al_7Cu_2Fe phase and the transformation of crystal orientation distribution compared with the HCC alloy (Fig. 4).

The mechanical properties and electrical conductivity are summarized in Table 2. The ultimate

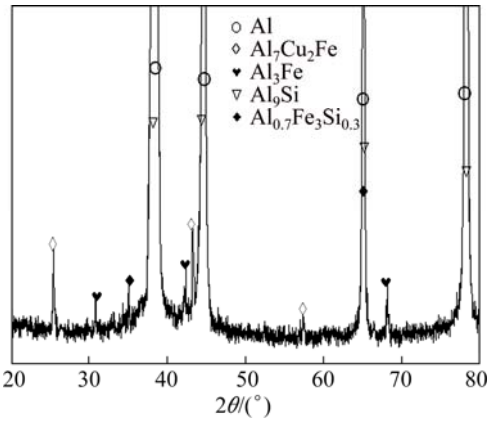

Fig. 6 XRD pattern of Conform processed Al−0.70Fe−0.24Cu alloy

Table 2 Mechanical properties and electrical conductivity of Al−0.70Fe−0.24Cu alloy conductors

Material	Ultimate tensile strength/ MPa	Elongation/ %	Electrical conductivity at 20 °C (%IACS)
HCC	93.5	21	57.13
Conform	135.3	25	60.61
CC&R	103−152	≥10	57.99

tensile strength, elongation and electrical conductivity of the HCC Al−0.70Fe−0.24Cu alloy are 93.5 MPa, 21% and 57.13% IACS (International annealed copper standard), respectively. While the ultimate tensile strength, elongation and electrical conductivity of the Conform processed Al−0.70Fe−0.24Cu alloy are all improved, which are 135.3 MPa, 25% and 60.61% IACS, respectively. The Conform process induces obviously refined and homogeneous microstructure, which leads to the improved mechanical properties of the processed alloy. The Conform process also induces the precipitation of Al_7Cu_2Fe phase, which causes the decrease of the content of solution atom, and therefore increases the electrical conductivity [8]. The properties of the processed alloy are better than the requirements of the Chinese specification (Designation: GB/T 3954) for the Al−0.70Fe−0.24Cu alloy conductor rods by CC&R. Therefore, it can be concluded that the proposed novel process could be used in the efficient production of Al−0.7Fe−0.24Cu alloy conductor with enhanced mechanical properties and electrical conductivity.

3.3 Creep behavior

3.3.1 Creep curve

The compressed creep curves of the Conform processed Al−0.70Fe−0.24Cu alloy conductor, annealed copper (T2) conductor and 1235 Al conductor crept at 90 °C and 76 MPa, are shown in Fig. 7. It can be seen that each creep curve consists of the primary creep stage

lasted for about 20 h and the steady-state creep stage lasted until the end of 100 h test. It is also noted that the creep strain rate is very high at the beginning of the primary creep stage and then gradually slows down to a steady-state creep rate for the Al−0.70Fe−0.24Cu alloy and annealed copper. While a visible creep strain increase is still observed during the steady-state creep stage for the high-stack-energy 1235 Al. The creep curves of Al−0.70Fe−0.24Cu alloy and annealed copper at 90 °C and 76 MPa almost level off during the steady-state creep stage due to the lack of recovery.

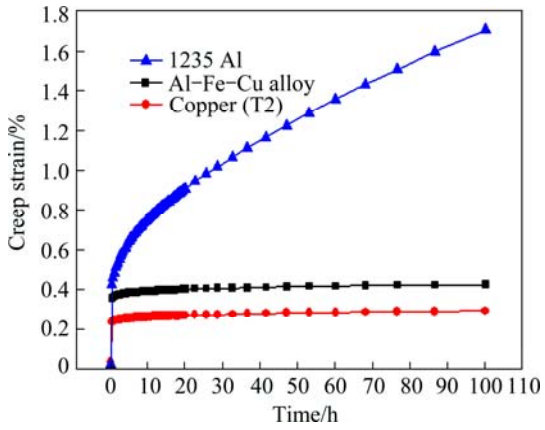

Fig. 7 Compressed creep curves of Al−0.70Fe−0.24Cu alloy, copper (T2) and 1235 Al at 90 °C and 76 MPa

Table 3 shows the creep strain after 100 h and the steady creep strain rate of the Al−0.70Fe−0.24Cu alloy, annealed copper and 1235 Al at 90 °C and 76 MPa. The creep strain of the Al−0.70Fe−0.24Cu alloy crept for 100 h is 1.446 times that of annealed copper and 25.1% of that of 1235 Al. The steady creep strain rate of the Al−0.70Fe−0.24Cu alloy is 8.2×10^{-10} s^{-1}, which is approximately equal to that of the annealed copper as well as only 29.71% of that of 1235 Al. Compared with the annealed copper and 1235 Al, it can be observed that the Conform processed Al−0.70Fe−0.24Cu alloy conductor exhibits favorable creep-resistant performance under the test conditions of 90 °C and 76 MPa.

Table 3 Creep strain and steady creep strain rate of Al−0.70Fe−0.24Cu alloy, copper (T2) and 1235 Al

Material	Creep strain/%	Creep strain rate/s^{-1}
Al−0.70Fe−0.24Cu	0.428	8.2×10^{-10}
Copper (T2)	0.296	8.1×10^{-10}
1235 Al	1.705	2.76×10^{-9}

3.3.2 Creep law

When a material is loaded under a constant stress at a constant temperature, it undergoes a time-dependent creep strain $\varepsilon(t)$. BARBER and CALLAGHAN [9] suggested a power law function of creep strain with time for improved overhead line conductors using 1120 Al. In cases where the creep strain and temperature are lower, the creep strain $\varepsilon(t)$ usually increases linearly with the logarithm of the time, which is called logarithmic creep [10]. NABARRO [10] proposed the mechanism of logarithmic creep: the work-hardening of a set of barriers to dislocation motion. In the work-hardening model, the creep rate $\dot{\varepsilon}$ is given by

$$\dot{\varepsilon}=\dot{\varepsilon}_0\exp[-U/(kT)] \tag{1}$$

The activation energy U is not constant in time, and T is the experiment temperature. The value of $\dot{\varepsilon}_0$ depends on the volume density of barriers. From the above equation, it follows that

$$\frac{\mathrm{d}\varepsilon}{\mathrm{d}t}=\dot{\varepsilon}_0\exp(-\frac{U_0+\lambda\varepsilon}{kT}) \tag{2}$$

The solution of Eq. (2) is

$$\varepsilon=(\frac{kT}{\lambda})\ln(1+\frac{t}{\tau}) \tag{3}$$

where

$$\tau=(\frac{kT}{\lambda\dot{\varepsilon}_0})\exp(\frac{U_0}{kT}) \tag{4}$$

Parameters kT/λ and τ are determined by the experiment condition. The data of the creep test are well fitted by the expression (Fig. 8):

$$\varepsilon_p=a\ln(bt+1) \tag{5}$$

where ε_p represents the primary creep strain. Parameters a and b respectively referring to kT/λ and τ are 1.175×10^{-4} and 3.705×10^{13}. The reliability coefficient is 0.99941, which indicates that the primary creep of the alloy complies with the logarithmic law of the work-hardening model.

The steady state creep strain ε_s fits to a linear relationship with time, given by

$$\varepsilon_s=c+dt \tag{6}$$

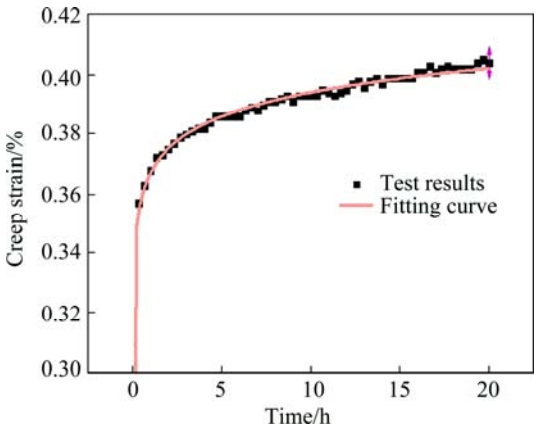

Fig. 8 Fitting curve of primary creep results of Al−0.70Fe−0.24Cu alloy

where parameter c is a constant and d is the steady creep strain rate.

3.3.3 Creep microstructure evolution

Figure 9 shows the TEM images of specimens crept for 20, 40 and 100 h. It has been observed that abundant movable dislocations exhibit in the Conform processed Al−0.70Fe−0.24Cu alloy (Fig. 5(b)). During the creep process, dislocations with the lowest activation energy are likely to move first upon the initial loading, thus, a high creep rate is observed at the beginning of the creep (Fig. 7). At the primary creep stage, dislocations tangle up (Fig. 9(a)) gradually. As time passes, network dislocations arise within the matrix (Fig. 9(b)) and cell walls tend to be formed (Fig. 9(c)). According to JAFFE and DORN [11,12], the cross-slip mechanisms are responsible for the room temperature creep of Al alloy. The movement of dislocations is uniquely characterized by cross-slip. The network dislocations observed in Figs. 9(b) and (c) obstruct the cross-slip of mobile dislocations. The mobile dislocations may interact with the network dislocations and become immobilized. Only the immobile dislocations that are trapped in the network dislocations contribute to the strain hardening of the material [13]. As a result of strain hardening, some movable dislocations decrease gradually, which slows down the primary creep rate. The mobile dislocations decrease and the immobile dislocations increase. According to dislocation dynamic, the creep strain rate is given by [14]

$$\dot{\varepsilon} = \rho_{\mathrm{m}} b v \tag{7}$$

where ρ_{m} is the mobile dislocation density, b is the Burgers vector and v is the dislocation velocity. Accordingly, the creep rate decreases with time. The test stress cannot reactivate the immobilized dislocations. The creep deformation exhibits a work-hardening feature due to the lack of recovery. The creep strain normally follows a logarithmic relationship with time in the work-hardening motion, which has been observed in the present study.

Tangled dislocations pinned by the plate and spherical phases also are observed in Fig. 9(d). The dislocations cannot bypass the phases by cross slip or climb mechanisms. Thus, the plate and spherical phases can effectively hinder the dislocation motion. Therefore, the creep resistance of the Al−0.70Fe−0.24Cu alloy is improved by the presence of particles [15]. According to the energy dispersion analysis (EDS) of the phase in Fig. 9(d), the phase is enriched with Al, Fe and Cu. The plate and spherical particles precipitated at the grain boundaries and sub-boundaries are AlFe and Al_7Cu_2Fe phases, respectively [16].

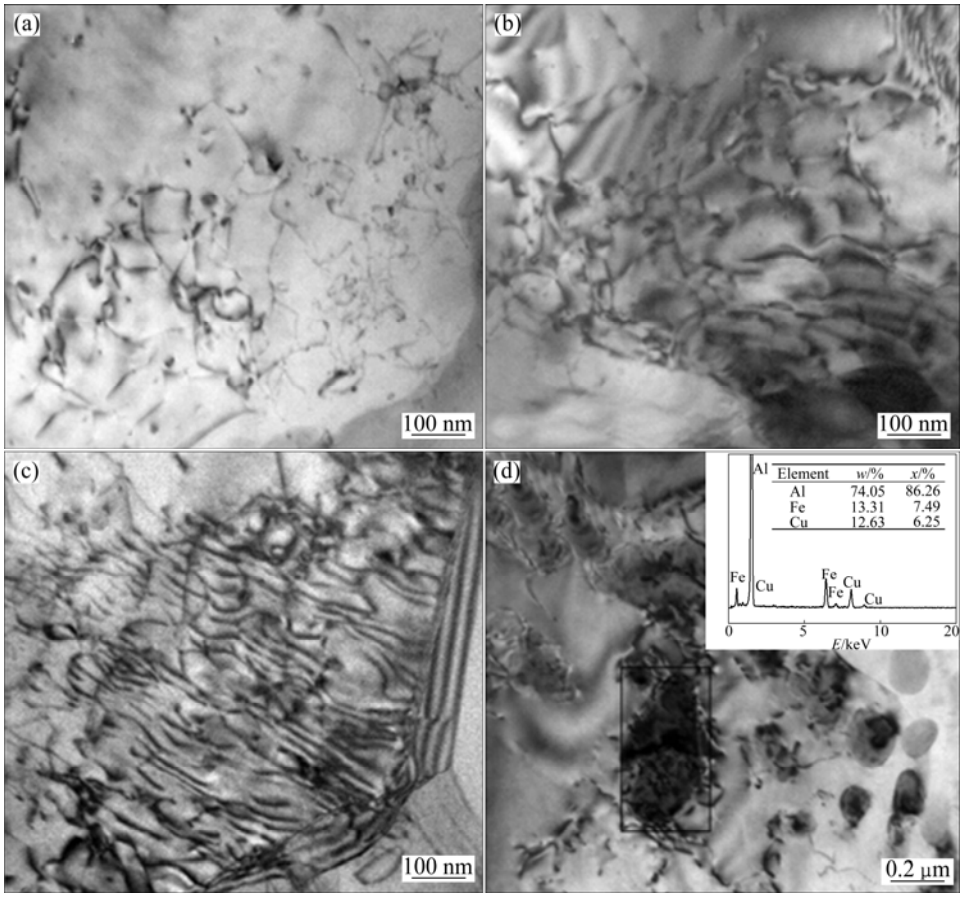

Fig. 9 TEM images of Al−0.70Fe−0.24Cu alloy crept at 90 °C and 76 MPa for different time: (a) 20 h; (b) 40 h; (c, d) 100 h

4 Conclusions

1) A novel process for manufacturing Al−0.70Fe−0.24Cu alloy conductor was proposed, which includes horizontal continuous casting and Conform process. The mechanical properties, electrical conductivity and the compressed creep behaviour at 90 °C and 76 MPa for 100 h were studied.

2) The Conform process induces obvious grain refinement, strain-induced precipitation of the Al_7Cu_2Fe phase and the transformation of crystal orientation distribution, which leads to the improved comprehensive properties.

3) The processed alloy has good combined mechanical properties and electrical conductivity. A better creep resistance under the conditions of 90 °C and 76 MPa is shown compared with pure Al and copper, and the primary creep strain may comply with the logarithmic law $\varepsilon_p=a\ln(bt+1)$ with fitting constants a and b of 1.175×10^{-4} and 3.705×10^{13}, respectively.

4) The enhanced properties are attributed to the grain refinement as well as the fine and homogeneously distribution of thermally stable AlFe and Al_7Cu_2Fe precipitation phases.

References

[1] McQUEEN H J, CHIA E H, STARKE E A. Fe-particle-stabilized aluminum conductors [J]. JOM, 1986, 38: 19−24.

[2] ENGLER O, LAPTYEVA G, WANG N. Impact of homogenization on microchemistry and recrystallization of the Al−Fe−Mn alloy AA8006 [J]. Materials Characterization, 2013, 79: 60−75.

[3] KIM M G, LEE G C, PARK J P. Continuous casting and rolling for aluminum alloy wire and rod [J]. Materials Science Forum, 2010, 638: 255−260.

[4] VERWIJS J P, WECKMAN D C. Influence of mold length and mold heat transfer on horizontal continuous casting of nonferrous alloy rods [J]. Metallurgical Transactions B, 1988, 19: 201−212.

[5] ZHANG Xiao-wei, HUANG Jin-feng, DENG Kang, REN Zhong-ming. Solidification of horizontally continuous casting of super-thin slab in stable magnetic field and alternating current [J]. Transactions of Nonferrous Metals Society of China, 2011, 21(1): 196−201.

[6] ZHANG H, JIANG F L, SHANG X Y, LI L X. Flow stress and microstructural evolution of the horizontal continuous casting Al−0.96Mn−0.38Si−0.18Fe alloy during hot compression [J]. Materials Science and Engineering A, 2013, 571: 25−32.

[7] GUAN Ren-guo, ZHAO Zhan-yong, CHAO Run-ze, LIAN Chao, WEN Jing-lin. Simulation of temperature field and metal flow during continuous semisolid extending extrusion process of 6201 alloy tube [J]. Transactions of Nonferrous Metals Society of China, 2012, 22(5): 1182−1189.

[8] GUO Lei, YI Dan-qing, ZHANG Bing, WANG Bin, LIU Hi-qun, LIU Gong-qi. Effect of extrusion ratio on microstructure and electrical properties of AA8030 aluminum alloy rod [J]. The Chinese Journal of Nonferrous Metals, 2013, 23(8): 2083−2089. (in Chinese)

[9] BARBER K W, CALLAGHAN K J. Improved overhead line conductors using aluminium alloy 1120 [J]. IEEE Transactions on Power Delivery, 1994, 10(1): 403−409.

[10] NABARRO F R N. The time constant of logarithmic creep and relaxation [J]. Materials Science and Engineering A, 2001, 309−310: 227−228.

[11] JAFFE N, DORN J E. Effect of stress on creep rate of high-purity aluminum in the cross-slip region [J]. Transactions of the Metallurgical Society of AIME, 1962, 224: 1167−1173.

[12] DORN J E, JAFFE N. Effect of temperature on the creep of polycaystalline aluminum by the cross-slip mechanism [J]. Transactions of the Metallurgical Society of AIME 1961, 221: 229−233.

[13] WANG S H, ZHANG Y G, CHEN W X. Room temperature creep and strain-rate-dependent stress-strain behavior of pipeline steels [J]. Journal of Materials Science, 2001, 36: 1931−1938.

[14] KIM H K. Low-temperature creep behavior of ultrafine-grained 5083 Al alloy by equal-channel angular pressing [J]. Journal of Mechanical Science and Technology, 2010, 24: 2075−2081.

[15] LIN Bo, ZHANG Wei-wen, CHENG Pei, WANG Xian-song, LI Yuan-yuan. Microstructure and mechanical properties of Al−5.0Cu−0.6Mn−0.5Fe alloy prepared by squeeze casting [J]. The Chinese Journal of Nonferrous Metals, 2013, 23: 1195−1201. (in Chinese)

[16] XING Z P, KANG S B, KIM H W. Microstructural evolution and mechanical properties of the AA8011 alloy during the accumulative roll-bonding process [J]. Metallurgical and Materials Transactions A, 2002, 33: 1521−1530.

水平连铸−连续挤压成形 Al−0.70Fe−0.24Cu 合金导线的显微组织和性能

张晓苑[1]，张 辉[1,2]，孔祥鑫[1]，傅定发[1,2]

1. 湖南大学 材料科学与工程学院，长沙 410082；2. 湖南大学 湖南省喷射沉积技术及应用重点实验室，长沙 410082

摘 要：提出一种制备 Al−0.70Fe−0.24Cu 合金导线的新工艺，该工艺包括水平连续铸造和随后的 Conform 连续挤压成形，并对合金的力学性能、导电性能和压缩蠕变性能进行研究。结果表明：Conform 连续挤压工艺导致明显的晶粒细化、应变诱导 Al_7Cu_2Fe 相的析出以及晶体取向分布的改变。采用该工艺加工的 Al−0.70Fe−0.24Cu 合金导线具有良好的综合力学性能和导电性能；在 90 °C 和 76 MPa 条件下，该合金与纯铝和退火铜相比具有良好的抗蠕变性能，蠕变初始阶段的应变与时间遵循对数关系。合金性能的提高与在加工过程中形成的细晶和均匀分布的 AlFe 及 Al_7Cu_2Fe 热稳相有关。

关键词：Al−0.70Fe−0.24Cu 合金；水平连铸；连续挤压成形；显微组织；性能

(Edited by Wei-ping CHEN)